Available at www.sciencedirect.com

ScienceDirect

journal homepage: www.elsevier.com/locate/he

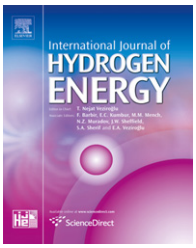

Autonomous BDFIG-wind generator with torque and pitch control for maximum efficiency in a water pumping system

P. Camocardi [a,b,*], P. Battaiotto [a], R. Mantz [a,c]

[a] LEICI, Universidad Nacional de La Plata, 1 y 47, CC 91 (1900) La Plata, Argentina
[b] CONICET, Argentina
[c] Comisión de Investigaciones Científicas de la Provincia de Buenos Aires, Argentina

ARTICLE INFO

Article history:
Received 30 November 2009
Received in revised form
22 December 2009
Accepted 18 February 2010
Available online 20 March 2010

Keywords:
Wind energy
Water pumping
Brushless doubly-fed induction generator
Dynamical sliding mode control
Pitch control

ABSTRACT

This paper presents and analyzes the operation strategy for an autonomous wind energy conversion system oriented to water pumping. It consists of a wind turbine with a Brushless Doubly-Fed Induction Generator (BDFIG), electrically coupled with a squirrel cage induction machine moving a centrifugal type water pump. Because of no brushes and slip rings, the BDFIG is suitable for autonomous systems, which often work in hard conditions. Additionally, the power flow on the BDFIG principal stator could be driven from a fractional power converter connected on the auxiliary stator winding. This Turbine-BDFIG and Motor-Pump configuration provides a high robustness and reliability, reducing the operational and maintenance costs. The operation strategy proposes, for wind speeds smaller than the rated, to maximize the volume of water pumped based on the optimization of the wind energy capture. To do that, a sliding mode control tracks the optimal turbine torque by means of a torque control. Meanwhile, for wind speeds greater than the rated, a pitch control keeps the water pump within the safe operation area by adjusting the speed and power of the turbine in their rated values. To assess and corroborate the proposed strategy, simulations with different wind profiles are made.

1. Introduction

Water supply is one of the principal problems in the development of remote regions. A recently proposed solution to this problem is the usage of autonomous water pumping systems with electrical coupling (generator–motor) between the wind turbine and the water pump [1]. With this coupling, the water pump location can be independently selected from the wind turbine location; therefore, the turbine could be placed in a site of optimum wind energy while the pump could be located near the water well, improving the system efficiency [2].

Among the different variable speed wind energy conversion systems intended for electric water pumping, there are three configurations that stand out. One of them takes advantage of the multi-pole Permanent Magnet Synchronous Generator, where a gearbox is not necessary. It presents direct coupling between the generator and motor stators, then the speed of both machines keeps a constant relationship. Its main drawback is that the components must be specially sized for every case [2]. The second configuration presents back-to-back electronic converters in the power channel that decouple the pump and turbine speeds. In this case the converters must be dimensioned to drive the rated

* *Corresponding author*. LEICI, Universidad Nacional de La Plata, 1 y 47, CC 91 (1900) La Plata, Argentina. Tel./fax: +54 221 4259306.
E-mail addresses: pcamocardi@ing.unlp.edu.ar (P. Camocardi), pedro@ing.unlp.edu.ar (P. Battaiotto), mantz@ing.unlp.edu.ar (R. Mantz).
0360-3199/$ – see front matter © 2010 Professor T. Nejat Veziroglu. Published by Elsevier Ltd. All rights reserved.
doi:10.1016/j.ijhydene.2010.02.099

pumping power, increasing the system cost [3]. There is a third type of configuration that uses Wound Rotor Asynchronous Generators with fractional power converters. Despite the reduced cost of the converters, it presents the disadvantage that both the generator and the gearbox require regular maintenance [4].

The Brushless Doubly-Fed Induction Generator (BDFIG) arises as an alternative to the Permanent Magnet and Wound Rotor machines in wind energy conversion systems [5]. It consists mainly of two stator windings magnetically coupled through a nested rotor cage [6]. Due to their operational and constructive characteristics, the BDFIG can work with low mechanical speeds allowing a considerable reduction in the gearbox relationship or even its elimination. Additionally, the absence of slip rings and brushes increases the system reliability and reduces the operational and maintenance costs, which are of great importance in autonomous systems [7].

The *wind operation area* of a wind energy conversion system can be divided into several regions depending on the wind speed, giving therefore, different control objectives for each area. When the wind speed is below its rated value, the objective is to extract all the available energy. This can be performed by operating the turbine in its optimal torque point. Meanwhile, when the wind speed is above its rated value, the most commonly used way to adjust the turbine aerodynamic torque is to control the pitch angle of the blades [8].

This paper presents the use of a Brushless Doubly-Fed Induction Generator in an autonomous wind conversion system for a water pumping application. For maximum efficiency, the operation strategy proposes a dynamical sliding mode control to track the optimal turbine torque by means of a torque control. Also, a pitch control loop provides power limitation at rated values, allowing the system to operate in a wide range of winds. Finally, simulations for different wind profiles and a discussion of the results are made.

2. System description

The system analyzed in this paper, and sized for a power of 75 kW, consists of a wind turbine with a BDFIG electrically coupled with a squirrel cage induction machine moving a centrifugal water pump (Fig. 1). The main power flow is controlled through the BDFIG auxiliary stator by changing the frequency and voltage of its excitation. For a better understanding of the system, it is broken up into three subsystems. The first one is mainly constituted by the Wind Turbine and the BDFIG, the second is comprised of the Water Pump and the Induction Motor, and the third subsystem includes the Electronic Converters.

2.1. *Wind turbine – brushless doubly-fed induction generator*

The BDFIG consists of two three-phase stator windings, named principal and auxiliary windings, magnetically coupled through a nested rotor cage [6]. The number of the pole pairs of each stator winding is chosen in order to avoid the direct transformer coupling between them. The BDFIG mathematical model can be find in the references: [7,9].

The BDFIG auxiliary stator is fed through a fractional power AC/AC frequency converter with a three-phase voltage of variable frequency (f_{as}). Thence, under steady-state condition, the principal stator angular frequency is given by:

$$\omega_{ps} = \left(p_p + p_a\right)\Omega_g - \omega_{as}, \tag{1}$$

with p_p and p_a the pole pairs of the principal and auxiliary windings, Ω_g the angular speed of the BDFIG shaft and ω_{as} the auxiliary stator angular frequency.

This operation mode allows the converter to control, from the auxiliary stator winding ($\omega_{as} = 2\pi f_{as}$), the principal stator frequency, decoupling it from the speed of the turbine-generator shaft.

The BDFIG is propelled by a wind turbine with three 6-m blades with variable pitch angle, coupled to the generator through a gearbox with a 1:2 speed ratio. The power and mechanical torque developed on the turbine shaft are given by the well-known equations [10]:

$$P_t = \frac{1}{2}\cdot\rho\cdot A\cdot C_p(\lambda,\beta)\cdot W^3, \tag{2}$$

$$T_t = P_t/\Omega_t, \tag{3}$$

with ρ the air density, A the blade swept area, W the wind speed, Ω_t the turbine shaft speed, $C_p(\lambda,\beta)$ the power coefficient, λ the tip speed ratio and β the pitch angle. The generic equation used to model the $C_p(\lambda,\beta)$, where the maximum value (called $C_{p\ max}$) is obtained for $\beta = 0$, is given by [11]:

$$C_p(\lambda,\beta) = c_1\left(\frac{c_2}{\lambda_i} - c_3\beta - c_4\right)e^{\frac{-c_5}{\lambda_i}} + c_6\lambda, \tag{4}$$

with:

$$\frac{1}{\lambda_i} = \frac{1}{(\lambda + 0.08\beta)} - \frac{0.035}{(\beta^3+1)}, \tag{5}$$

and c_1 to c_6 characteristic coefficients of the turbine.

Fig. 2 shows a family of torque-speed curves for different winds and $\beta = 0$. The dashed line (T_{opt}) represents the geometric locus of optimal torque where the power delivered by the turbine for every wind speed is maximal.

In order to rotate the blades of the wind turbine around its longitudinal axis, they have a device called pitch actuator. This type of actuators, of non-linear characteristics, can be hydraulic or electro-mechanical and allow the implementation of reliable and efficient control strategies for power or speed limitation. In closed loop, the pitch actuator can be modeled as a first-order dynamic system with saturation in the amplitude and derivative of the output signal [12]. The dynamic behavior, in its linear region, is described by the differential equation:

$$\dot{\beta} = -\frac{1}{\tau}\beta + \frac{1}{\tau}\beta_c, \tag{6}$$

with τ the actuator time constant, and β_c the desired value of β.

The basic dynamic equation that represents the behavior of the *Turbine-BDFIG* subsystem, by assuming that the mechanical dynamics is dominant with respect to the electrical and neglecting the viscous damping, is given by:

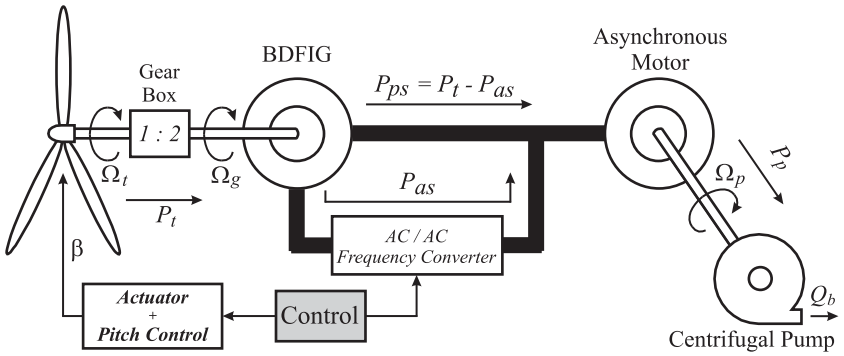

Fig. 1 – Proposed system scheme.

$$\dot{\Omega}_t = \frac{T_t' - T_g}{J_{t+g}}, \tag{7}$$

with T_t' the turbine torque referred to the generator shaft side, T_g the electrical torque of the BDFIG and J_{t+g} the turbine and generator inertia moment.

2.2. *Water pump – induction motor*

Due to practical issues like robustness, costs and maintenance, induction machines are usually employed for propelling the centrifugal pump [13]. Hence, the pumping unit has a 75 kW asynchronous motor with 2 pole pairs ($p_m = 2$) and squirrel cage rotor, mechanically coupled to a centrifugal pump of equivalent power. Under steady-state operation, the power and mechanical torque of the pump are given by (Fig. 2) [9]:

$$P_p = k_p \cdot \Omega_p^3, \tag{8}$$

$$T_p = P_p/\Omega_p = k_p \cdot \Omega_p^2, \tag{9}$$

with k_p the pump constant and Ω_p the pump shaft speed. The mechanical motor speed is controlled at constant flux, by its feeding frequency. Because the coupling is electrical, this frequency is the electrical frequency of the BDFIG principal stator winding (f_{ps}). Assuming that the induction motor slip is small, we can express its electro-mechanical torque as:

$$T_{im} = k_{im}(\Omega_{ps} - \Omega_p), \tag{10}$$

with k_{im} the torque-speed constant and $\Omega_{ps} = \omega_{ps}/p_m$. Thereby, speed and power of the pump can be directly controlled by the principal stator frequency.

With the same considerations made for the turbine-generator dynamics, the basic dynamic equation that represents the behavior of the *Pump-Induction Motor* subsystem is:

$$\dot{\Omega}_p = \frac{T_{im} - T_p}{J_{im+p}}, \tag{11}$$

with J_{im+p} the motor and pump inertia moment.

2.3. *Electronic converters*

To control the main power flow, the system has an AC/AC frequency converter constituted by two bidirectional electronic converters in back-to-back configuration, rated at only a fraction of the wind turbine rating [5,9].

The *auxiliary stator side converter* modifies, by means of two control loops, the auxiliary stator voltage and frequency to

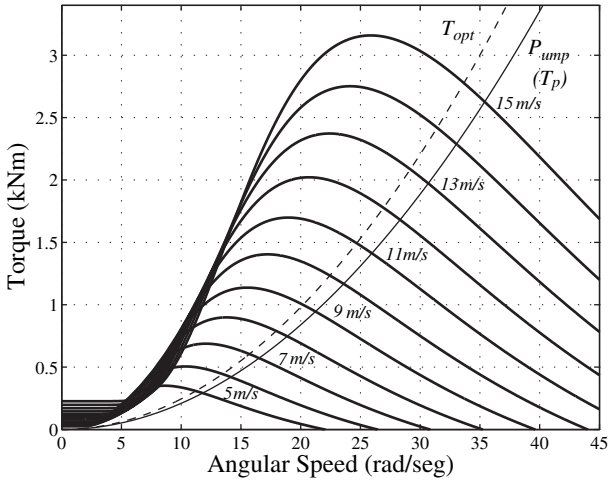

Fig. 2 – Wind turbine torque–speed curves for $\beta = 0$, referred to the generator shaft side.

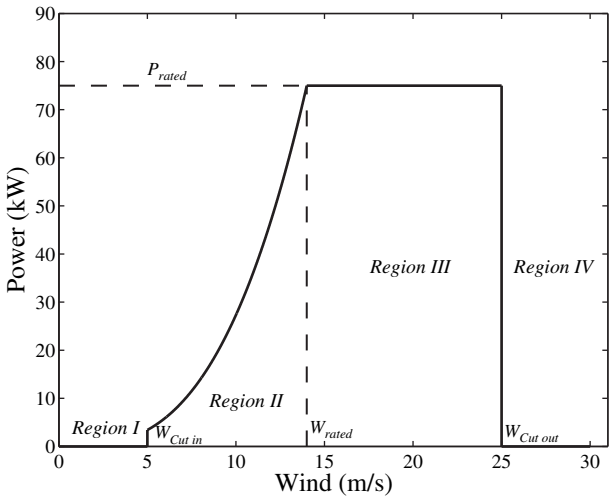

Fig. 3 – Ideal power curve and operation regions.

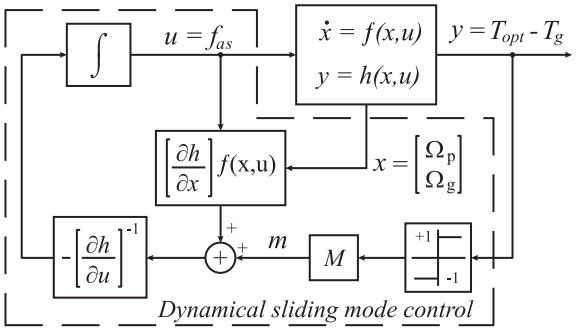

Fig. 4 – Dynamical sliding mode control scheme.

change the power pump consumption, keeping the principal stator V/f ratio constant. The auxiliary stator power value, P_{as}, results as a consequence of these control actions.

The *principal stator side converter* allows a bidirectional power flow between the auxiliary and principal stators, and therefore the maximal power transfer to the pump.

Because of the BDFIG electrical torque is a function of the load power consumption, an expression for T_g can be derived from the power balance between the generator power ($P_g = T_g \cdot \Omega_g$) and the induction motor power ($P_{im} = T_{im} \cdot \Omega_{ps}$), by assuming ideal electronic converter efficiencies:

$$P_g = T_g \cdot \Omega_g = P_{im} = T_{im} \cdot \Omega_{ps}, \tag{12}$$

$$\therefore T_g = (\Omega_{ps}/\Omega_g) \cdot T_{im}. \tag{13}$$

Then, substituting (1) in (13) yields:

$$T_g = \frac{(p_p + p_a)}{p_m} \cdot T_{im} - \frac{2\pi f_{as}}{p_m \cdot \Omega_g} \cdot T_{im}. \tag{14}$$

3. Control strategy

For a wind turbine, the *generation capacity* specifies how much power can be extracted from the wind taking into consideration both physical and economic limitations. It is usually represented with a *power generated–wind speed* curve, and is called *ideal power curve* (Fig. 3). The operational range of winds, as can be seen, is delimited by the cut-in ($W_{Cut\text{-}in}$) and the cut-out ($W_{Cut\text{-}out}$) winds. The turbine remains stopped beyond these limits. Below the cut-in wind speed (*Region I*), the system does not work due to the different components losses are comparatively higher than the available energy in the wind. Above the cut-out wind speed (*Region IV*) the turbine is disconnected in order to avoid structural damage due to the overload that they produce. Within these margins, there are

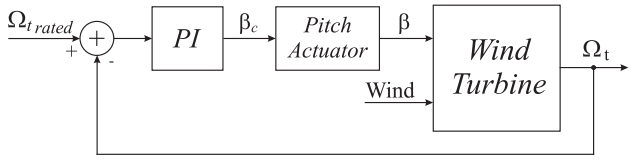

Fig. 5 – Pitch control strategy for power limitation.

two regions with different generation objectives (*Region II* and *Region III*).

In *Region II*, the available power in the wind is lower than the rated power. For that reason, the generation objective in this interval is to take out all the available energy from the wind. In order to do that, and as it will be show later, a torque control loop tracks the optimal torque curve of the turbine (T_{opt}), where the power at each wind speed is maximum.

On the other side, the goal in the region of large wind speeds (*Region III*) is to limit the generated power at the rated power, and thus to avoid the overload of the system components. Therefore, the turbine should be operated with an efficiency lower than the $C_{p\ max}$. Thus, a pitch control adjusts the turbine torque so that the Turbine-BDFIG subsystem operates at rated speed ($\Omega_{t\ rated}$), delivering the rated power. In the following sections, the system operation in the last two regions are analyzed, while the work conditions for *Region I* and *Region IV* are not discussed in this work.

3.1. *Torque control – Region II*

The main control target is to maximize the volume of water pumped based on the optimization of the wind energy capture. To do that, the pumping unit should present on the generation subsystem a load that allows the turbine to operate with maximum energy conversion efficiency. Because of the difficulties and inaccuracies which introduce the wind speed measurement in the wind turbine vicinity, the use of this information is avoided. Thence, a torque control that follows the turbine optimal torque for every wind speed condition is implemented, where the reference torque value is obtained from the BDFIG speed (Ω_g). The loop compares T_{opt} with the generator electric torque (T_g) and modifies the auxiliary stator frequency (f_{as}), controlling in this way the principal stator frequency (f_{ps}), and hence, the power pump consumption.

Taking into account the dynamic coupling between the pumping unit and the generation system, and the non-linear

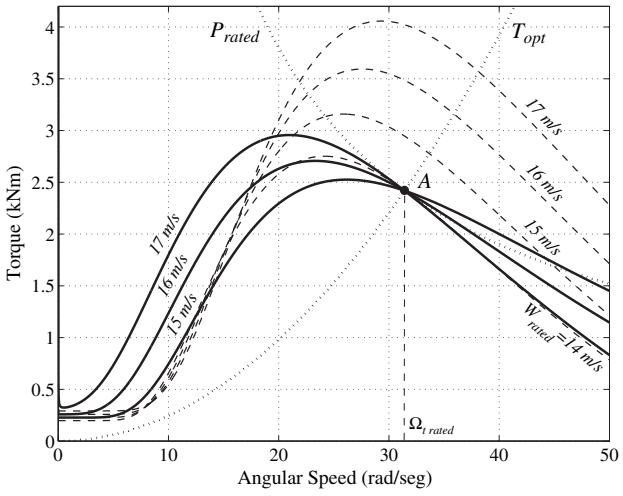

Fig. 6 – Wind turbine torque–speed curves with (continuous line) and without (dashed line) pitch control, for wind speeds greater than the rated.

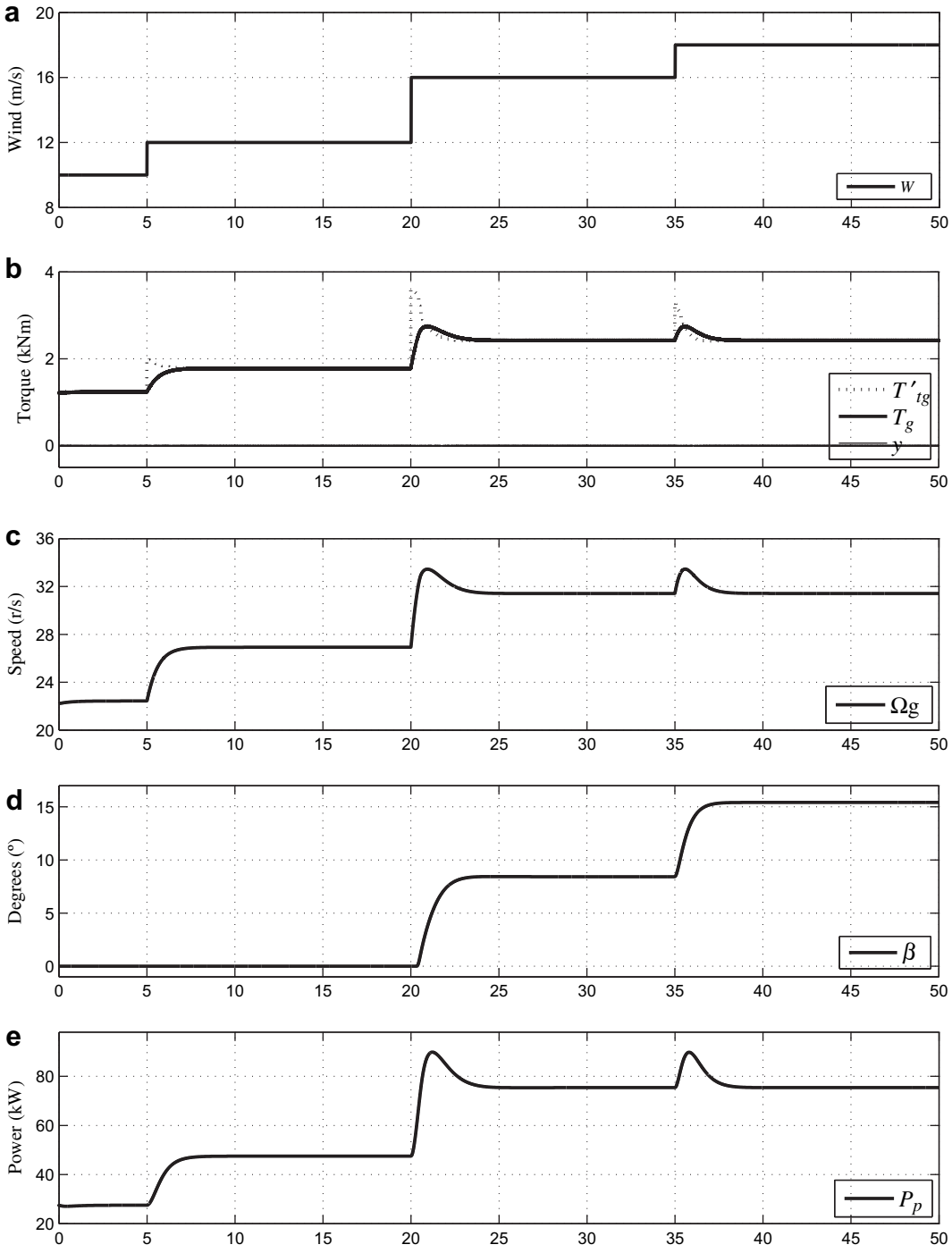

Fig. 7 – Simulation results for step wind profile.

dynamics involved, the design of a controller to ensure stability and a good behavior dynamics in the full range of winds is not a simple task. With the idea of overcoming these limitations, the torque control loop is developed using a Sliding Mode Control (SMC).

In general terms, the SMC presents some distinctive properties with respect to other control schemes such as: the closed loop response becomes insensitive to some model parameter uncertainties, the dynamic behavior may be tailored by the particular choice of the sliding function, and simplifies the control in non-linear systems [14]. The control objective is expressed through the sliding surface by:

$$y = h(x, u) = T_{opt} - T_g, \tag{15}$$

with x the variable states (Ω_p and Ω_g) and u the action control (f_{as}).

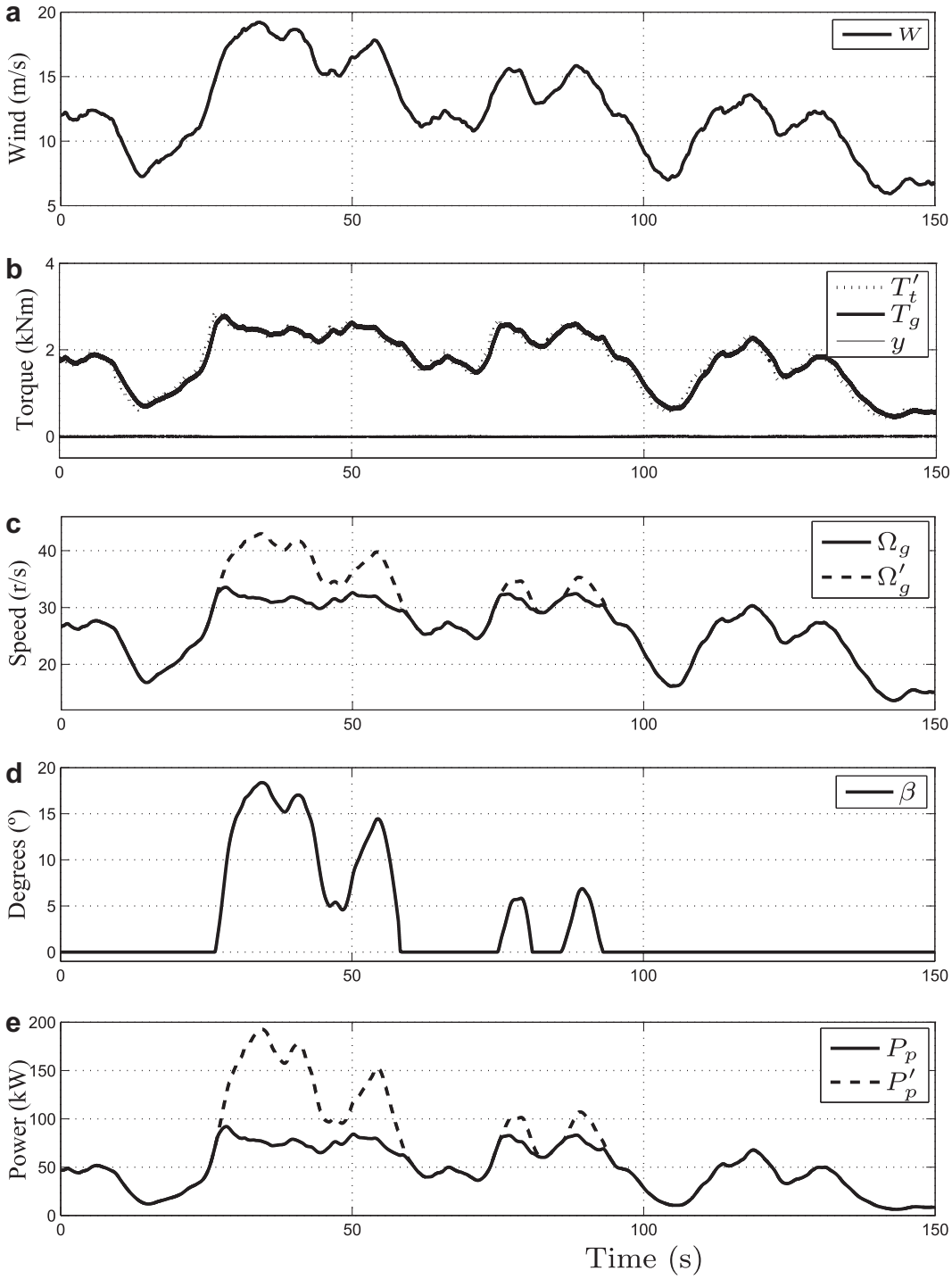

Fig. 8 – Simulation results for real wind profile.

In conventional SMC, to remain on the sliding surface ($h(x, u) = 0$), the structural changes are made over the control variable u. This signal jumps between two extreme control values in such a way that the system sees a mean value known as equivalent control (u_{eq}), which allows to stay on the surface [14]. Obviously, the discontinuous action of the conventional SMC cannot be applied in a direct way over the value of the auxiliary stator frequency (f_{as}). Thus, a Dynamical Sliding Mode Control (DSMC) is proposed, by imposing the autonomous dynamics on the output of the system [3,15]:

$$\dot{y} = -M\,\mathrm{sign}(y), \tag{16}$$

where the different sign between the sliding surface and its derivative guarantees that y always tends to zero, reaching and remaining on the sliding surface.

Then, deriving (15) and computing the required control signal u for the previous task yields:

$$\frac{du}{dt} = \left[\frac{\partial h}{\partial u}\right]^{-1} \left\{ \left[\frac{\partial h}{\partial x}\right] f(x,u) + M \operatorname{sign}[h(x,u)] \right\}. \quad (17)$$

In this way, (16) not only ensures the convergence of the control objective, but it does so with a smooth action of control (f_{as}). A block diagram depicting the expanded system with the dynamical discontinuous feedback control scheme, stated in (17), is shown in Fig. 4.

3.2. *Pitch control – Region III*

Fig. 5 shows a typical pitch control scheme with the aim of limiting the generated power of the turbine, in *Region III*. The shaft speed is compared with the turbine rated speed. The error signal is taken by the *PI* controller, which gives the desired value of the pitch angle (β_c).

In this way, the controller adjusts the turbine speed at the rated speed, allowing the turbine to deliver the P_{rated} at a wind speed bigger than the rated (W_{rated}). This situation can be seen in Fig. 6, which shows the turbine curves for wind speeds greater than the rated, both for the case with $\beta = 0$ (dashed line) and for $\beta \neq 0$ (continuous line). It can be noticed how correctly adjusting β for different wind speeds, the turbine can be operated at $\Omega_{t\ rated}$ and P_{rated} (Point A).

4. Simulation results

Results of the proposed strategy for the autonomous wind energy conversion system are presented in this section. The simulations were carried out using the Matlab/Simulink environment. The first wind velocity profile (W) employed to highlight the system and control features is shown in Fig. 7a, and consists of steps at 10, 12, 16 and 18 m/s. Although these data do not correspond to a real profile, steps are a standard testing signal which permit a clear interpretation of system behavior.

Fig. 7b and c shows the torque and speed of the turbine-BDFIG subsystem working in sliding mode. Also, the output of the system (y) is displayed in Fig. 7b. Notice that this signal remains in zero throughout the simulation verifying the sliding mode system operation. That condition guaranties that the controlled variable (T_g) always follows the reference (T_{opt}) changes. For wind speeds greater than W_{rated} (16 and 18 m/s), the pitch control adjusts the turbine torque (T'_t) so that the system operates at $\Omega_{t\ rated}$ and the water pump does not consume, in steady state, a power greater than the rated.

Fig. 8 shows the same set of curves that the Fig. 7, but for a real wind profile, with gusts that exceed the W_{rated}. They also show, in dashed line, the turbine speed (Ω'_t) and the pump power (P'_p) without the pitch control to limit the power. It can be seen the conditions that would be exposed the system components, with long periods of work outside of the safe operation area.

From the two figures can be noticed that the system maximizes the volume of water pumped based on the optimization of the wind energy capture, and limits the generated power of the turbine through the control of its speed. With that, the generator and the pumping subsystem are not overloaded when the wind speed exceeds the rated.

5. Conclusions

An autonomous wind energy conversion system using a BDFIG for water pumping was presented. The absence of slip rings on the BDFIG and the possibility of reducing or even eliminating the gearbox increase the system reliability and reduce the maintenance and the operational costs. The proposed configuration with direct generator–load electric coupling and auxiliary stator control reduces the converter sizing and the whole system cost, while improving its performance. A control strategy for maximum efficiency operation, divided into different work regions depending on the turbine shaft speed, was proposed. The system operation was evaluated for different wind conditions showing the proposed strategy advantages both for the optimal torque tracking of the turbine and for the power limitation through the pitch control.

Acknowledgments

This work was supported by the Argentine Institutions: UNLP, CONICET, Fundación YPF, ANPCyT and CICpBA.

REFERENCES

[1] Velasco M, Probst O, Acevedo S. Theory of wind-electric water pumping. Renewable Energy 2004;29:873–93.
[2] Muljadi E, Nix G, Bialasiewicz J. Analysis of the dynamics of a wind-turbine water-pumping system. in: Proceedings of the 2000 power engineering society summer meeting, IEEE, vol. 4; 2000, p. 2506–19.
[3] Fernández D, Mantz R, Battaiotto P. Sliding mode control for efficiency optimization of wind-electrical pumping systems. Wind Energy 2003;6(2):161–78.
[4] Pena R, Clare J, Asher G. A doubly fed induction generator using back-to-back PWM converters supplying an isolated load from a variable speed wind turbine. Electric Power Applications, IEE Proceedings 1996;143(5):380–7.
[5] Li H, Chen Z. Overview of different wind generator systems and their comparisons. Renewable Power Generation, IET 2008;2(2):123–38.
[6] Williamson S, Ferreira A, Wallace A. Generalized theory of the brushless doubly-fed machine: part 1 and 2. Electric Power Applications, IEE Proceedings 1997;144: 111–29.
[7] Rüncos F. Modelagem, projeto e análise de máquinas assíncronas trifásicas duplamente alimentadas sem escovas. Ph.D. dissertation, Univ. Fed. de Santa Catarina; 2006.
[8] Mantz R, De Battista H. Hydrogen production from idle generation capacity of wind turbines. International Journal of Hydrogen Energy 2008;33(16):4291–300.
[9] Camocardi P, Battaiotto P, Mantz R. Brushless doubly fed induction machine in wind generation for water pumping.

In: Proc. Int. Conf. Elec. Mach. 2008 (ICEM08); 2008, ISBN: 978-1-4244-1736-0.
[10] Fernández F, Battaiotto P, Mantz R. Impact of wind farms voltage regulation on the stability of the network frequency. International Journal of Hydrogen Energy 2008;33(13):3543–8.
[11] Heier S. Grid integration of wind energy conversion systems. John Wiley & Sons Ltd; 1998.
[12] Bianchi F, De Battista H, Mantz R. Wind turbine control systems. Springer; 2007.
[13] Fiaschi D, Graniglia R, Manfrida G. Improving the effectiveness of solar pumping systems by using modular centrifugal pumps with variable rotational speed. Solar Energy 2005;79(3):234–44.
[14] Utkin V, Guldner J, Shi J. Sliding mode control in electromechanical systems. Taylor & Francis; 1999.
[15] Sira-Ramirez H. On the dynamical sliding mode control of nonlinear systems. International Journal of Control 1993;57: 1039–61.